Toxicogenomics: A New Paradigm for Nanotoxicity Evaluation

9

Sourabh Dwivedi, Quaiser Saquib, Bilal Ahmad, Sabiha M. Ansari, Ameer Azam, and Javed Musarrat

Abstract

The wider applications of nanoparticles (NPs) has evoked a world-wide concern due to their possible risk of toxicity in humans and other organisms. Aggregation and accumulation of NPs into cell leads to their interaction with biological macromolecules including proteins, nucleic acids and cellular organelles, which eventually induce toxicological effects. Application of toxicogenomics to investigate molecular pathway-based toxicological consequences has opened new vistas in nanotoxicology research. Indeed, genomic approaches appeared as a new paradigm in terms of providing information at molecular levels and have been proven to be as a powerful tool for identification and quantification of global shifts in gene expression. Toxicological responses of NPs have been discussed in this chapter with the aim to provide a clear understanding of the molecular mechanism of NPs induced toxicity both in in vivo and in vitro test models.

Keywords

Nanoparticles · Toxicogenomics · Oxidative stress · RNA-Seq · Microarray

S. Dwivedi · A. Azam
Department of Applied Physics, Faculty of Engineering and Technology, Aligarh Muslim University, Aligarh, Uttar Pradesh, India

Q. Saquib
Zoology Department, College of Sciences, King Saud University, P.O. Box 2455, Riyadh 11451, Saudi Arabia

B. Ahmad
Department of Agricultural Microbiology, Faculty of Agricultural Sciences, Aligarh Muslim University, Aligarh, Uttar Pradesh, India

S. M. Ansari
Department of Botany and Microbiology, College of Sciences, King Saud University, P.O. Box 2455, Riyadh 11451, Saudi Arabia

J. Musarrat (✉)
Department of Agricultural Microbiology, Faculty of Agricultural Sciences, Aligarh Muslim University, Aligarh, Uttar Pradesh, India

Department of Biosciences and Biotechnology, Baba Ghulam Shah Badshah University, Rajouri, Jammu and Kashmir, India
e-mail: musarratj1@yahoo.com

Q. Saquib et al. (eds.), *Cellular and Molecular Toxicology of Nanoparticles*, Advances in Experimental Medicine and Biology 1048, https://doi.org/10.1007/978-3-319-72041-8_9

9.1 Introduction

Nanoparticles (NPs) have been defined as materials having at least one dimension in the nanoscale (1–100 nm), bearing size-dependent physiochemical properties different than their bulk counterparts. NPs have high surface-to-volume ratio, which provide them high reactivity and physicochemical dynamicity. The advantageous properties of more complex NPs retain the potential to drawn enormous research from different fields for its application in medical diagnostics and treatments [1]. Several commercially available consumer products contains NPs, particularly in cosmetics and sunscreens [2]. NPs have also been utilized in different areas of biology and medicine including tissue engineering, drug and delivery formulations, for hyperthermia induced tumor destruction, DNA structure probes and biosensors [3–5]. Nonetheless, there are uncertainties that the unique properties of NPs may also pose potential health risks in the occupationally and non-occupationally exposed populations [2].

With the greater demand of NPs, there is huge ambiguity related to their potential hazards towards environment and its different trophic levels. Special concerns have been raised on NPs mediated release of metal ions, reactive oxygen species (ROS) or its direct reactivity towards biological membranes [6, 7]. A major key question persisting with NPs toxicity is whether it is linked with the general properties shared by varying NPs or is it specific to individual NPs. Considering these facts, if toxicological effects are related to shape, agglomeration or the size of NP, then similar toxicological effects can be expected for different NPs [8]. On the other hand, if NPs composition controls the interaction, then definite toxicity would be expected [9, 10]. An understanding of the toxicological effects of each NPs is critical for any prediction of their immediate and long-term risks for humans upon occupational and consumer goods exposure (Fig. 9.1).

Exposure to NPs may occur during its production via handling, aerosolization may also occur during energetic processes, such as vortexing, weighing, sonication, mixing and blending [11]. Hence, inhalation is considered a relevant route of exposure [11, 12]. Presence of the NPs in the body may induces pathophysiological changes that might contribute to the development of cancer [13], cardiovascular diseases [14], respiratory tract inflammation [15], neurodegenerative diseases [16], and many other pathologies [17]. Researchers have summarized the potential mechanisms of nanotoxicity via greater ROS level and induction of inflammatory responses such as Parkinson's disease [18]. NPs can also alter the permeability of blood brain barrier and re-translocate from the site of deposition to other parts of the body via circulatory or lymphatic system [19]. The actual prophecy of the adversity of NPs cellular exposure and uptake are still lacking [20]. Cells can rapidly alter its transcriptomic output (gene expression profile) in response to extracellular and intracellular environmental changes, and get adapted for their survival and function. Nonetheless, biological functions and normal physiological activities can get disturbed under excessive environmental changes. Consequently, profiling of gene expression has been proven helpful in recognizing the NPs toxicity and its relevant molecular mechanism [21–25]. Application of toxicogenomics in NPs research can significantly contribute to unravel the mechanistic action of toxicity, parallel to traditional approaches and other omic technologies. Quantitation of mRNA transcripts in NPs treated cells not only provide the mechanistic information, rather it also provides "genetic fingerprinting" from the pattern of gene expression that the NPs elicit in vitro and in vivo. In this chapter, we have discusssed the cellular toxicity of NPs and the importance of toxicogenomics approaches in nanotechnology and NPs induced alterations in transcriptomic profile reportedly studied based on the RNA-Seq, and microarray techniques.

9.2 Toxicogenomics in Nanoparticles Research

Several biomarkers including mRNA transcripts, protein and enzyme expressions have been widely applied as health indicators for the range

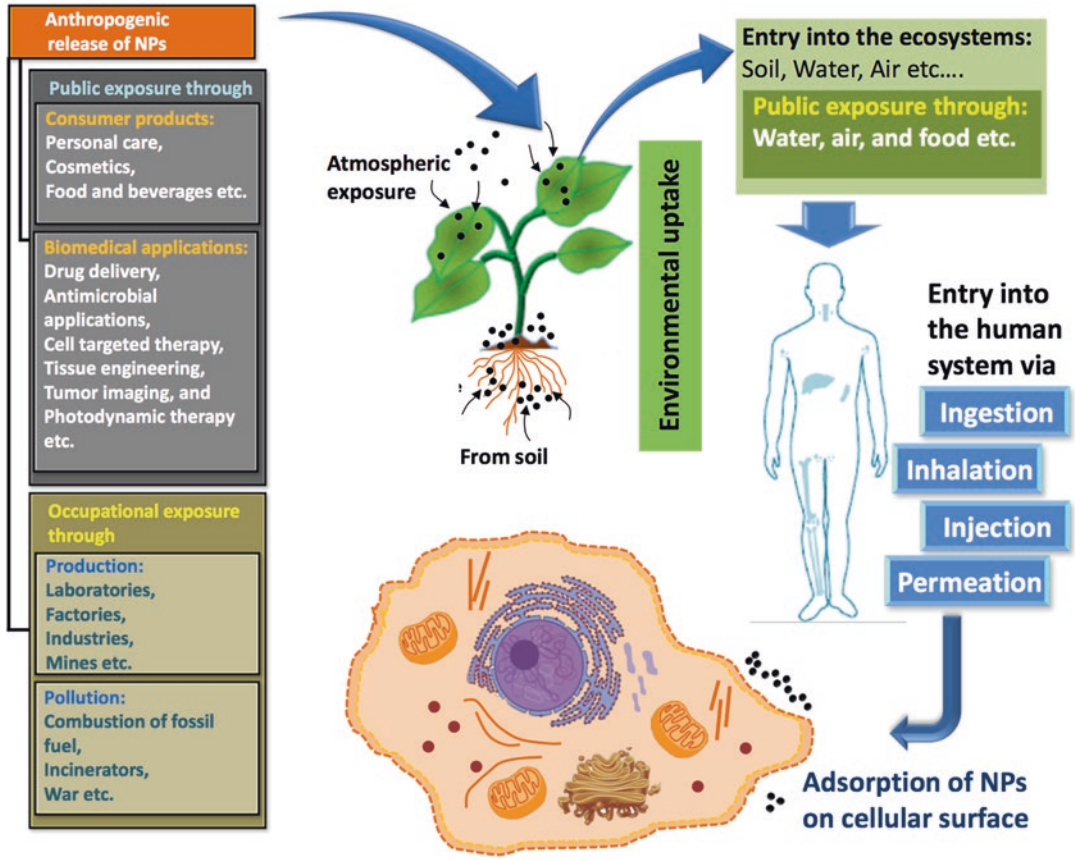

Fig. 9.1 Cellular interaction and uptake of natural and anthropogenic NPs

of human diseases, also it has been utilized to examine the xenobiotics induced changes in the health status of different model and non-model organisms [26–28]. The technology is based on the principle that the mRNA that codes for proteins, are expressed differently in an unexposed organism, vis-a-vis the xenobiotic exposed organisms. The quantification of genome-wide mRNA level by transcriptomic approaches involve the techniques like RNA sequencing (RNA-Seq) and oligonucleotide hybridization (microarray). Toxicogenomics, primarily comprising the hybridization technologies, has been a preferred choice in modern toxicological research. The vast data output and pathway based information represents toxicogenomics as a powerful approach, which has been used now for over decades for identifying novel mechanism of toxicity, disturbance in vital biological pathways, as well as biomarkers of toxicity [6]. In fact, the imperative benefit of toxicogenomics is the holistic approach, which provides a platform for discerning the genetic level changes from the perspective of altered pathways and networks revealing the novel mechanisms of toxicity and toxic responses (Fig. 9.2).

9.3 Nanoparticles Toxicity Analysis by RNA-seq

RNA-seq, being a novel and state-of-the art technique, allows the robust quantification of RNA transcripts on a genome-wide level [29]. Several properties of RNA-seq viz. accuracy and higher dynamic range allow detection of alternative splicing, and no preexisting knowledge of the genomic sequence makes it more advantages

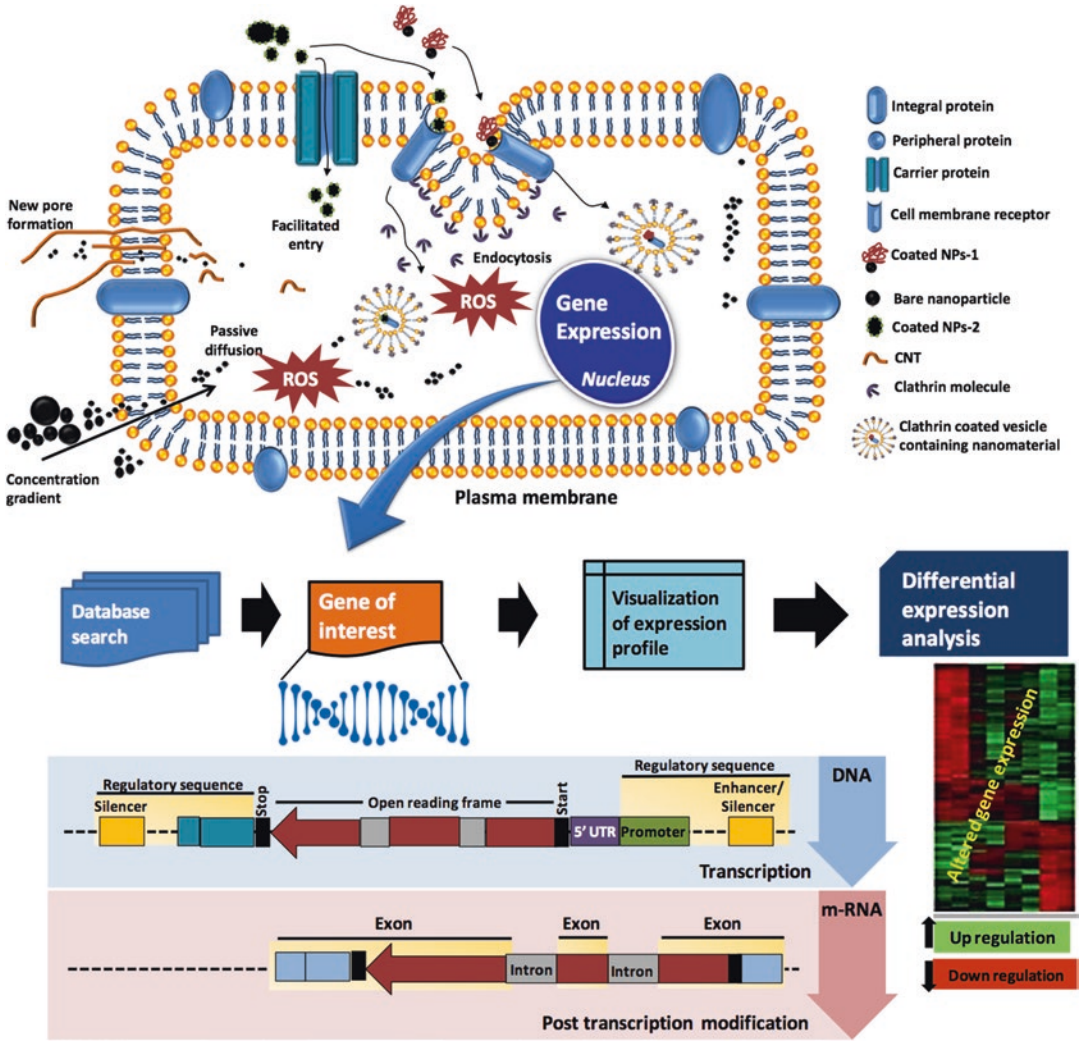

Fig. 9.2 Toxicogenomic approaches for evaluation of NPs toxicity

over microarray [29]. Consequently, the RNA-seq has recently gain entry into the field of nano-toxicology, bound to supersede microarrays in the toxicogenomics field [30]. RNA-seq can generate vast inventory of gene transcripts employing bioinformatics, DNA sequencing and sequence databases [29]. The low-abundance transcripts (approximately 30% of most transcriptomes) can easily be quantified by RNA-seq, also the technique can identify splice junctions and novel exons. RNA-seq accuracy and precision is equally comparable to quantitative real-time PCR [31, 32]. Data from various test models revealed that, about 40% changes in the protein level can be easily explained by knowing the mRNA abundance [33, 34]. Therefore, the application of RNA-seq based transcriptome profiling in NPs toxicity can provide detailed and substantial information, which can complement the results of other approaches.

The RNA-seq analysis of eukaryotic green alga *Chlamydomonas reinhardtii* exposed to metallic NPs (Ag, TiO_2, ZnO and CdTe/CdS quantum dots) revealed specific and different

effects. Of the 1.2×10^8 total reads, 5.0×10^7 (42%) mapped uniquely with a maximum of two mismatches and no deletions or insertions. *Chlamydomonas reinhardtii* exposed to TiO_2, ZnO, Ag-NPs and quantum dots (QDs) exhibited 96, 156, 141 and 49 upregulated genes, whereas 80, 29, 86 and 55 genes were found downregulated. NPs exposure (TiO_2, ZnO, and QDs) increased the levels of transcripts encoding subunits of the proteasome, suggesting proteasome inhibition, which is regarded as inducer of several major diseases, including Alzheimer's disease, and used in chemotherapy against multiple myeloma [35]. The RNA-seq analysis of MCF-7 cells treated with fullerene derivative too exhibited strong negative effect on a number of fundamental and interconnected biological processes involved in cell growth and proliferation, mainly including mRNA transcription, protein synthesis/maturation, and cell cycle progression. Comparatively, a fullerene derivative-1 in the same study exhibited no cytotoxicity, although some pathway overlaps were observed with a another fullerene derivative-2 (Fig. 9.3).

Gene ontology (GO) analysis of fullerene derivatives reveled the repression of transcriptional activators (*DHX9, NR2F1, GATA4, AHR*), pre-mRNA complex components (*HNRNPM, WDR77, POP1*) and the transcription elongator factor elongin A (*TCEB3*). Ribosome biogenesis was negatively affected, also the three fundamental genes of pre-rRNA (*RRP9, BOP1, UTP20*) responsible for the maturation and two major subunits of RNA polymerase III (*POLR3B, POLR3G*) were found down regulated. The down regulation of mentioned genes also repressed the protein synthesis, particularly the maturation (*SEC11C, SRPRB*) involved in the recognition and processing of signal peptide. In addition, molecular chaperones responsible for the folding of newly synthetized proteins, including *HSP70* (*HSPA1A, HSPA8*) and *HSP90* (*HSP90AA1*) were down regulated [36].

RNA-seq of nano-hybrid (made of a gold nanoparticle core and a peptide coating; P12) treated human peripheral blood mononuclear cells (PBMNC) exhibited anti-inflammatory effects. Global gene expression of PBMNC exposed to P12 revealed suppression of 233 genes upregulated by LPS stimulation, and 29 genes downregulated by LPS. Overall, ca. 40% of genes that were upregulated by LPS in human PBMNC were suppressed by P12 (Fig. 9.4).

P12 exposure resulted in the activation of different signalling pathways including PKR, interferon, TLR, chemokine, JAK-STAT and TNF [37]. Deep sequencing-based RNA-seq analysis indicated 45 differentially expressed genes in living *Hydra vulgaris*, when exposed to SiO_2-NPs. Among these genes, 29 transcripts were upregulated (2-fold to 25-fold) and 16 were downregulated (2.2-fold to 5-fold). The authors have concluded that a sizeable number of genes remain unknown, providing a valid source of functional information to be further investigated [38]. Fifth instar of silkworm (*Bombyx mori*) when exposed to TiO_2-NPs exhibited differential expression of 11,268 genes in the silkworm fat body, out of which 341 genes showed significant differences, among which 138 were upregulated and 203 were downregulated (Fig. 9.5I). The GO map exhibited eleven biological processes accounting >10% of the annotated genes related to metabolic, cellular and single-organism process showing the highest percentages of annotated genes. Five cellular component subgroups >10% of annotated genes having cell, cell part and organelle showing the highest percentages of annotated genes. Three molecular functions related to binding, catalytic activity and structural molecular activity accounted for 10% or more of annotated genes have been observed in the silkworm (Fig. 9.5II). Further processing the RNA-seq data by KEGG (Kyoto Encyclopedia of Genes and Genomes) scatterplots indicated significant enrichments of all differentially expressed genes. The major affected pathways by TiO_2-NPs exposure in silkworm, includes insulin signaling pathway, which mediate primarily in insect growth and development, nutrient metabolism, lipids and carbohydrates homeostasis and protein synthesis (Fig. 9.5III) [39]. Transcriptome study on the effects of Ag^+ and Ag-NPs in earthworm *Eisenia fetida* employing RNA-seq reveled that Ag^+ verses control yielded 529 and 618 downregulated and upregulated transcripts. *Eisenia fetida*

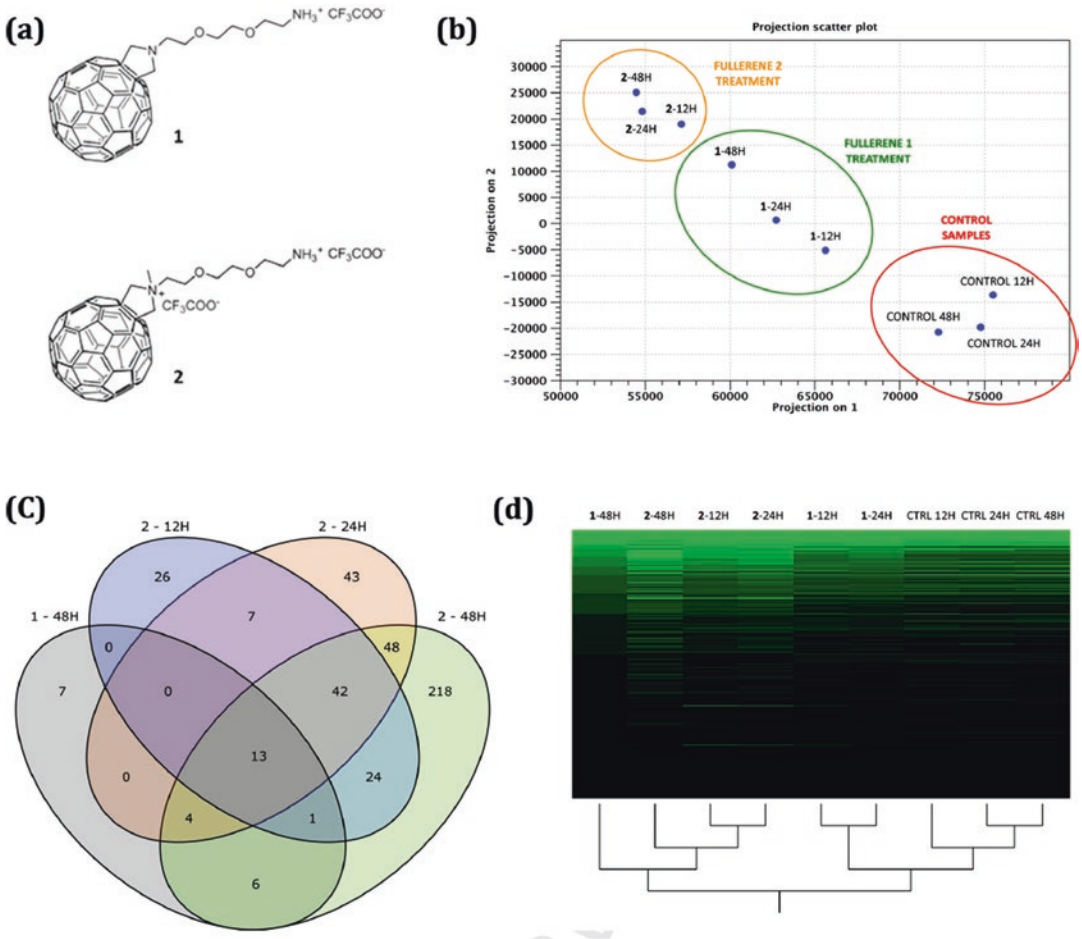

Fig. 9.3 (**a**) Structures of the two fullerenes *1* and *2*. (**b**) Principal component analysis showing the relationship between gene expression profiles of the six fullerene-treated and of the three control samples; a compound-dependent effect is visible, with fullerene 1 leading to minor effects compared to 2, as well as a time-dependent progressive deviation from the control samples. (**c**) Venn diagram depicting the differentially expressed genes identified by the Kal's Z-test on proportions common to the different experimental time points. (**d**) Hierarchical clustering of samples (Euclidean distance, complete linkage) based on the RNA-seq gene expression profiles (Reprinted from Toxicology, volume 314, Lucafò et al. [36], Profiling the molecular mechanism of fullerene cytotoxicity on tumor cells by RNA-seq, pages 183–192. Copyright (2013), with permission from Elsevier. See the reference list for full citation of proper credited)

exposed to Ag-NPs verses control exhibited 237 and 454 downregulated and upregulated transcripts, while Ag-NP verses Ag^+ showed 449 and 758 downregulated and upregulated transcripts. These alterations were related with the toxicity through pathways related to sugar and protein metabolism, disruption of energy production, ribosome function, molecular stress and histones gene alteration [40].

9.4 Microarray Analysis of Nanoparticles Toxicity

Microarrays analysis of genome changes is based on the probe, which is a pre-prescribed set of tens of thousands of genes at once. Comparative to RNA-seq, microarray is relatively cheaper, allowing multiple comparisons across treatments or individuals within an experiment. The transcrip-

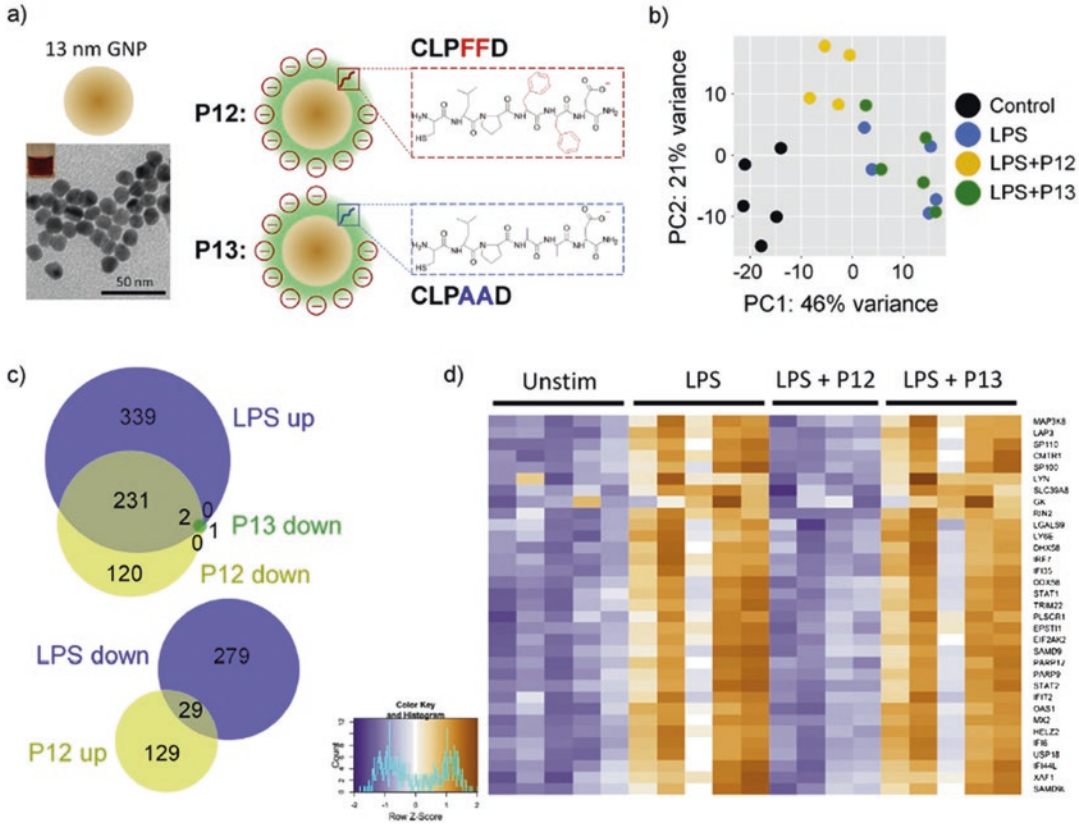

Fig. 9.4 Impact of anti-inflammatory nanoparticle P12 treatment on RNA-Seq transcriptome analysis of LPS-stimulated human PBMC. (**a**) Novel peptide-decorated nanoparticle hybrids with different surface chemistry (P12 vs. P13). (**b**) PCA plot. (**c**) Venn diagrams. (**d**) Differential expression profiles of top 33 genes ($p < 2.6 \times 10^{-15}$ and fold change >1.5) (Reprinted from Biomaterials, volume 111, Yang et al. [37], Endosomal pH modulation by peptide-gold nanoparticle hybrids enables potent anti-inflammatory activity in phagocytic immune cells, pages 90–102, Copyright (2016), with permission from Elsevier. See the reference list for full citation of proper credited)

tomic profiling using GeneChip or microarray technique allow the analysis of global gene expression in NPs exposed and unexposed test models. Exposure of retinoblastoma cell line (Y-79) with etoposide loaded NPs formulations modulated its gene activity. Microarray analysis exhibited differential expression of genes, showing upregulation of 171 genes, while 280 genes were found downregulated. The upregulated genes were mostly belonging to three groups including apoptosis, cell cycle and cell differentiation, and cell migration [41]. Time dependent (24 h and 48 h) exposure of zebrafish embryo with Ag-NPs, Ag-bulk, and Ag^+ exhibited differential expression of genes in the microarray analysis. After the 24 h post fertilization, embryos treated with Ag-NPs, Ag-bulk, and Ag^+ exhibited 35%, 71% and 89% of downregulated genes, while 65%, 29% and 11% genes were found upregulated. After 48 h of post fertilization 57%, 43%, 61% of genes were downregulated, and 43%, 57% and 39% genes were upregulated. The most significant over-represented in GO terms and KEGG pathways in all treatments at 24 h and 48 h were ribosome and oxidative phosphorylation. The prominent overlaps revealed that the toxicity of Ag-NP and Ag-bulk to zebrafish embryos has been predominantly associated with the toxicity of free Ag^+ [25]. The microarray analysis of human THP-1 derived macrophages exposed to single walled carbon nano tubes (SWCNT) reveled statistical significance of gene

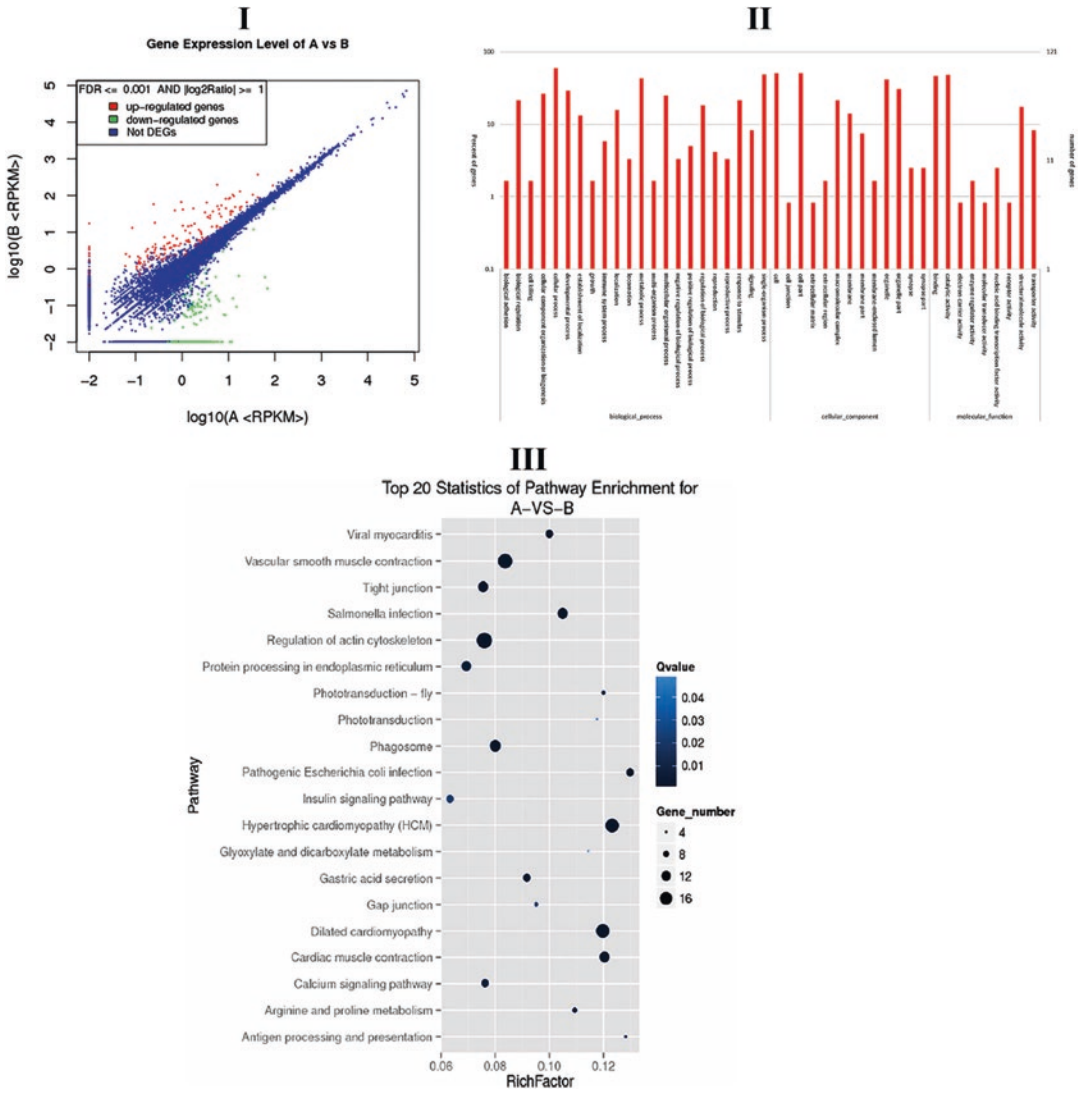

Fig. 9.5 (**a**) Statistical chart of significantly differentially expressed genes. A- represents the control group, while B- represents the experimental group. *RPKM* indicates the gene expression in samples. Red represents the upregulated genes in the figure; green represents downregulated genes; blue represents genes without significant differences. (**b**) Functional classification of significantly differentially expressed genes. A- represents the control group while B- represents the TiO_2-NP treatment group. The right ordinate represents the number of genes, with the maximum value of 121 indicating that a total of 121 genes underwent GO function classification. The left vertical axis represents the percentage of genes, indicating the percentage of functional genes to all annotated genes. (**c**) Scatter plot of KEGG pathway enrichment statistics. A- represents control group, and B- represents experimental group. Rich factor is the ratio of numbers of differentially expressed genes annotated in this pathway term to the numbers of all genes annotated in this pathway term. Greater rich factor means greater intensiveness. Q-value is corrected P-value ranging from 0 to 1, with a lower value means greater intensiveness. Top 20 pathway terms enriched are displayed in the figure (Adopted from Figs. 9.1, 9.2, and 9.3 of Tian et al. [39] (Copyright and Permission granted from the Biology Open Journal under the terms of the Creative Commons Attribution License (http://creativecommons.org/licenses/by/3.0), which permits unrestricted use, distribution and reproduction in any medium provided that the original work is properly attributed) (See the reference list for full citation of proper credited)

expression. Authors have analyzed the abundance changes in 406 pathways archived in KEGG and BioCarta databases. Microarray data exhibited significant alterations of at least 23 different vital pathways in SWCNT treated THP-1 derived macrophages. Considering the network data, authors have suggested that SWCNT uptake into macrophages activated the nuclear factor κB (NF-κB) and activator protein 1 (AP-1), leading to oxidative stress, proinflammatory cytokines activation, recruitment of leukocytes, induction of apoptotic genes and T cells [42].

In the same connection, human macrophage cell line exposed to 5 and 100 nm Ag-NPs were analyzed for approximately 28,000 cDNA profiles using GeneChip(R). Array profile revealed the expression of 45 genes between 5 nm Ag-NPs and the control, and 30 genes between 5 and 100 nm Ag-NPs. The stress genes (*HSP, HO, MT*) and one cytokine gene (*IL-8*) were the top expressed genes in 5 nm Ag-NPs treated cells. Also, the expression of *HO1, HSP*-70 and *MT-1E* RNA was significantly increased as the log2 ratio >2.0. *IL-8* was the only cytokine gene that was significantly induced among more than 70 cytokines [43]. Whole genome microarray analysis of the early gene expression changes induced by 10 and 500 nm amorphous silica NPs exhibited that the magnitude of change for the majority of genes affected were more tightly correlated with particle surface area, rather than either particle mass or number. The microarray data exhibited significant alteration of 503 and 502 genes by at least two-fold with either 10 or 500 nm silica NPs. The union of these gene sets included 753 genes, with 252 genes overlapping between the two particle size groups. Genes which were highly affected are known to play important role in lung inflammation, including *Cxcl2, Ccl4* (*MIP-1β*) and *Ccl3* (*MIP-1α*), along with the chemokine receptor *Cxcr4*. Nonetheless, gene set enrichment analysis revealed that among 1009 total biological processes, none were statistically enriched in one particle size group over the other [44]. Global gene expression of 11 nm dimercaptosuccinic acid (DMSA)-coated Fe-NPs on two cells (THP-1 and HepG2) revealed differential responses. Within ten top upregulated genes, Fe-NPs treated THP-1 cells induced maximum upregulation of *Cxcl13*, a humoral immune response gene. Other immune response genes upregulated were *Adamdec1*, *Ly96, Ifi44l*, *Ebi3*, *Clec7a*. While, in HepG2 cells treated with low and high doses of Fe-NPs induced maximum upregulation three genes (*Ifi27*, *Tagln and Ifi6I*) (Fig. 9.6I). Four way Venn diagram revealed that two genes (*Ddx58* and *Ifi27*) were commonly induced by low and high doses of FeNPs in both cell lines (Fig. 9.6IIa). Eleven genes (*Ddx58*, *Ifi44*, *Fbxo16*, *Parp9*, *Ifit3*, *Serpini1*, *Ifi27, Nexn*, *Usp25, Rg9mtd2 Ccne2*) were commonly induced by low dose of FeNPs in both cell lines. On the other hand, ten genes (*Tmed2, Ifi27, Ddx58, Akap12, Nampt, Narg1, Usp16, Ifi6, Col9a2, and Zcchc2*) were commonly induced by high dose of Fe-NPs in THP-1 and HepG2 cells. However, no genes were commonly repressed at both doses of Fe-NPs in the cell lines (Fig. 9.6IIb). The authors also developed a heat map of top 55 genes commonly regulated in these two cell lines. The hierarchical clustering revealed that these genes were classified into four clusters. Some genes were steadily upregulated or down-regulated in both types of cells, indicating cell-independent effects. Whereas some genes were inversely regulated in the two cell lines, suggesting cell-specific effects of the Fe-NPs (Fig. 9.7I). Interestingly, the authors have reported that Fe-NPs significantly enrich the hepatitis C pathway at both doses of treatments in the THP-1 cells (Fig. 9.7II) [45].

Kedziorek et al. [21] have examined the genome changes in *LacZ*-expressing mouse NSC cell line C17.2 exposed to superparamagnetic iron oxide nanoparticles (SPIONs). Microarray analysis of 2695 probe sets, representing 1399 genes, revealed that genes belonging to molecular functions of the cell describing activities such as catalytic reactions or binding that occur at the molecular level were significantly affected by the SPIONs exposure. A significant change in 970 genes of cellular function, 299 genes of gene expression, 312 genes of developmental, 431 genes of biologic regulation and 685 genes belonging to metabolic processes, have been reported. The treated cells also exhibited significant alterations in genes belonging to secretion,

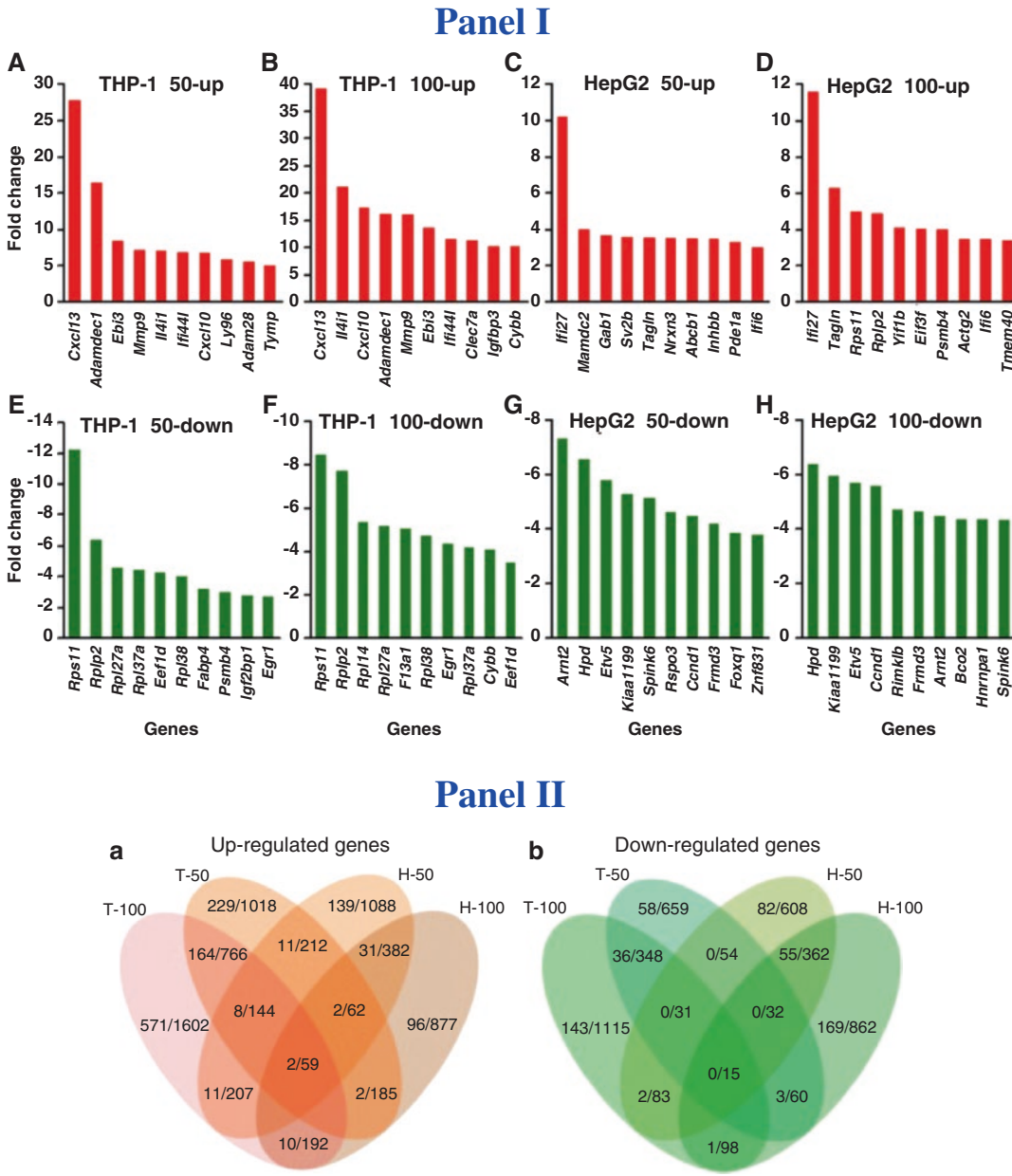

Fig. 9.6 *Panel I* showing the top 10 genes with the highest expression changes in the two cell types after treatment with Fe-NPs. (**a**, **b**) Induced genes in the THP-1 cells. (**c**, **d**) Induced genes in the HepG2 cells. (**e**, **f**) Repressed genes in the THP-1 cells. (**g**, **h**) Repressed genes in the HepG2 cells. 50-up and 100-up: induced genes in cells treated with 50 μg/mL and 100 μg/mL of FeNPs, respectively; 50-down and 100-down: repressed genes in cells treated with 50 μg/mL and 100 μg/mL of FeNPs, respectively. Some uncharacterized genes with fold changes greater than the lowest fold changes in these plots are not shown in this figure. *Panel II* Comparison of FeRGs in the THP-1 and HepG2 cells. **a** Comparison of induced genes in the two cell lines. **b** Comparison of repressed genes in the two cell lines. Each Venn diagram is divided into four areas labeled as T-50, T-100, H-50 and H-100. T-50 and T-100, THP-1 treated with 50 μg/mL and 100 μg/mL of FeNPs, respectively. H-50 and H-100, HepG2 cells treated with 50 μg/mL and 100 μg/mL of FeNPs, respectively. The number in overlapped area represents the overlapping genes. The numbers before and after the slash represent the genes with fold changes greater than 2 and 1.5, respectively (Reused from Figs. 9.3 and 9.4 of Zhang et al. [45] (Copyright and Permission granted from the Journal of Nanobiotechnology under the terms of the Creative Commons Attribution License (http://creativecommons.org/licenses/by/4.0), which permits unrestricted use, distribution, and reproduction in any medium, provided the original work is properly credited) (See the reference list for full citation of proper credited)

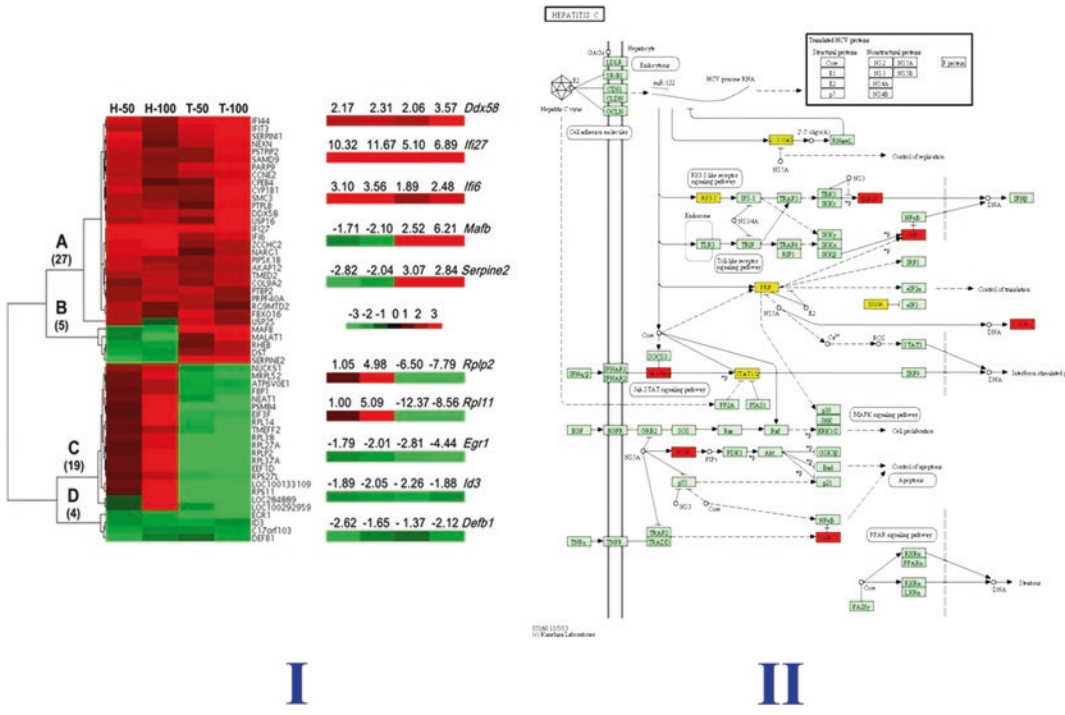

Fig. 9.7 (**I**) Cluster analysis of genes. Fifty-five FeRGs from the two cell lines were clustered according to their expression levels using a hierarchical clustering. The heatmap was drawn with Java TreeView. Red and green represent up- and down-regulation, respectively. The color depth reflects the expression level between −3 and +3 (marker). The numbers of genes in Clusters *A* to *D* are shown in parentheses. The fold changes of ten representative genes in four clusters are shown in the zoomed images. (**II**) KEGG pathway of hepatitis C in the FeNP-treated THP-1 cells. The genes in red refer to the FeRGs induced by 100 μg/mL of FeNPs. The genes in yellow refer to the FeRGs induced by both 50 μg/mL and 100 μg/mL of FeNPs. Abbreviations for the KEGG parameters can be found on the KEGG pathway webpage (Reused from Figs. 9.6 and 11 of Zhang et al. [45] (Copyright and Permission granted from the Journal of Nanobiotechnology under the terms of the Creative Commons Attribution License (http://creativecommons.org/licenses/by/4.0), which permits unrestricted use, distribution, and reproduction in any medium, provided the original work is properly credited) (See the reference list for full citation of proper credited)

transport, locomotion, reproductive processes, and establishment of localization. In addition, the expressions of heme oxygenase 1 (*Hmox1*) and transferrin receptor 1 (*Tfrc*) were repressed, while, genes responsible for detoxification (*Clu, Cp, Gstm2, and Mgst1*) and lysosomal function (*Sulf1*) were upregulated at later time points. Liu and Wang [24] have studied changes in the global gene expression of mouse macrophage (RAW264.7 cells) exposed to DMSA-Coated Fe_3O_4-NPs using GeneChips Mouse Genome 430 2.0 microarrays. The GO analysis revealed that several molecular functions and biological processes pertaining to metal ion transmembrane transporter activity, especially Fe ion transmembrane transporter activity and Fe ion binding, were significantly enriched in all DEGs. *Tfrc*, *Trf*, and *Lcn2* genes important to iron metabolism were frequently found in the GO terms. The microarray data of lung epithelial cell line (A549) exposed to 12.1 μg/ml Ag-NPs (EC20) for 24 and 48 h exhibited altered gene regulation of more than 1000 genes (>2-fold), while considerably fewer genes responded to Ag^+ (133 genes). The upregulated genes were belonging to the members of heat shock protein, metallothionein and histone families [23]. Human skin fibroblasts (HSF42) and human embryonic lung fibroblasts (IMR-90), both untransformed cells were exposed to multiwalled carbon nanotubes

(MWCNTs) and multiwalled carbon nano-onions (MWCNOs) exhibited profound gene expression changes, analyzed on new generation Affymetrix HTA GeneChip system. The low doses of both materials induced expressional changes in genes of secretory pathway, protein metabolism, golgi vesicle transport, fatty acid biosynthesis, and G_1/S transition of mitotic cell cycle. Also, an additional group of genes, involved in protein ubiquitination was found upregulated. Contrarily, high doses upregulated the genes in tRNA aminoacylation and amino acid metabolism pathways. Genes of inflammatory and immune response were also found upregulated [46].

BV2 microglia, which is an immortalized mouse cell line, when exposed to a mixture of anatase (70%) and rutile (30%) TiO_2-NPs (Degussia P25) exhibited global gene expressional changes in the microarray. The core canonical analysis reveled that BV2 exposed to P25 upregulated the signaling processes involved in B-cell death, ERK/MAPK receptors, apoptosis, calcium, and inflammation. P25 up-regulated the inflammatory (*NF-κB*), cell cycling and pro-apoptotic toxicity pathways. Core analysis of P25 induced downregulation of genes exhibited alteration of adaptive change and key energy production pathways, mainly associated with hypoxia, peroxisomes, and *Nrf2*-mediated oxidative stress [47]. In microarray analysis, male Sprague-Dawley rats fed with Synthetic Amorphous Silica (SAS) and NM-202 (a representative nanostructured silica for OECD testing) for 24 and 84 days exhibited non significant gene alteration in jejunal epithelial samples and liver homogenates. Although, fibrosis-related gene expression was significantly affected for NM-202 treated animals after 84-days of exposure, but not for SAS treated animals [48]. Osmond-McLeod et al. [49] demonstrated the transcriptome changes by the application of NPs based sunscreens. Mice treated with both the TiO_2-NPs sunscreen and UVR exposure (TiO_2-NPs + UVR) showed very low levels of differential regulation, as compared to untreated mice (Control-UVR) (14 genes). Pathway analysis exhibited that three of the top 5 canonical pathways in TiO_2-NPs + UVR were linked with metabolic functions (Heme Biosynthesis II; Tetrapyrrole Biosynthesis II; Mevalonate Pathway I). In addition, breast cancer regulation Stathmin1 and circadian rhythm signalling were also affected in the canonical pathways. While, ZnO-NPs sunscreen with UVR (ZnO-NPs + UVR) and ZnO-NPs sunscreen without UVR (ZnO-NPs-UVR) did not showed any transcriptome alterations [49].

HaCaT cells exposed to tungsten carbide (WC) and tungsten carbide cobalt (WC-Co) NPs exhibited whole genome transcription alterations. Fluorescence signal of microarray in all treatments revealed 1956 upregulated and 1146 downregulated differentially expressed genes, with more than two-fold expression level. HaCaT cells exposure to $CoCl_2$ salt, as metal source of Co induced strongest changes in the gene expression (373 and 826 genes for 3 h and 3 day) followed by WC-Co (37 and 248) and WC-NPs (28 and 49), respectively. Data analysis by enrichment method exhibited the fact that differentially expressed genes were related to hypoxia, endocrine pathways, carbohydrate metabolism, and targets of several transcription factors [50]. Human lung epithelial cells (A549) exposed to silica-NPs exhibited a dose dependent response, ranging from 5 to 2258 significantly differentially modulated transcripts compared with controls, with a fold change of at least 1.5 and p-value <0.05. Canonical analysis exhibited the coagulation system and intrinsic and extrinsic prothrombin activation pathways as most highly altered. Additionally, the acute phase response, xenobiotic metabolism, TREM1 signaling pathways and oxidative stress response were altered. The authors have extended the transcriptome into exproteome to understanding the NPs effect on proteins. Heat-shock proteins (*HSP70* and *HSP90*), detoxification enzymes such as glutathione reductase (*GSR*), glutathione S-transferase (*GSTP1*), lactate dehydrogenase (*LDH*A), peroxiredoxins (*PRDX*1, *PRDX6*), thioredoxin reductase (*TRXR1*), protein disulfide isomerase (*PDIA6*), and aldo-keto reductases (*AKR1B1*, *AKR1B10*, *AKR1C1/C2*, and *AKR1C3*) were found as affected proteins in the exproteome analysis [51]. Human intestinal epithelium model (Caco-2) cell line, when exposed to pristine

(surface untreated) CeO_2-NPs exhibited 1643 modified genes. Comparatively, the manufactured CeO_2 Nanobyk™ NPs in the same study have not affected the gene regulation, while 344 and 428 modified genes were found for light (NB-DL) and acid (NB-DA) degraded CeO_2 Nanobyk™ NPs. Pristine CeO_2-NPs exhibited changes in the cellular growth and proliferation (274 genes) and cell death (265 genes) biological process. The canonical pathway analysis of pristine CeO_2-NPs revealed that it alters the mitochondrial function through the under expression of 27 genes of complexes I, III, IV and V [52]. Fisichella et al. [53] in their previous study on pangenomic oligomicroarrays (4 × 44,000 genes) demonstrated that TiO_2-STNPs have not altered the gene expression of Caco-2 cells when exposed to the highest concentration of 10 μg/ml.

Al_2O_3-NPs exposed human bronchial epithelial (HBE) cells significantly increased expression of 54 genes and decreased expression of 304 genes. GO analysis unravel the fact that total genes encoding proteins necessary for mitochondrial function were differentially expressed. KEGG pathway enrichment analysis of these 27 genes of mitochondrial function and neural system disease were significantly enriched. *NDUFA2, NDUFS, NDUFC2, NDUFA1, NDUFA4, UQCR11 (complex III), COX7B, COX17* (complex IV) and *ATP5H* (complex V, F0 unit) were among the most affected genes (Fig. 9.8) [54].

Global gene expression in the HepG2 cells upon 20 and 50 nm Ag-NPs treatment exhibited differential regulation of genes. After short exposure of 4 h, the 20 nm Ag-NPs induced alterations of 811 genes, out of which 649 were upregulated and 162 were downregulated. Comparatively, the 50 nm Ag-NPs treatment induced stark difference, only 21 genes were altered and all of them were upregulated. Extended exposure of 24 h did not made any massive alterations in the gene expression by both sizes of Ag-NPs. Overlapping of DEGs exhibited alterations of five common genes after 4 and 24 h of 20 nm Ag-NPs exposure, including members of the metallothionein (MT) family (*MT1B, MT1F, MT1G, MT1M* and *MT2A*). The 50 nm Ag-NPs exposure also showed four common genes of MT family, except an additional activation of SOX4 gene. Overall, *MT1B* and *MT1M* were shared by all treatment groups. Out of 108 GO terms derived from the 649 upregulated genes in 4 h 20 nm of Ag-NPs revealed 23 categories, on top listed the metabolism (47%), development (19%), protein metabolism (15%), cell differentiation (13%), biosynthesis (11%), death (9%) and cell communication (9%). The 162 downregulated genes exhibited 21 groups of GO terms enrichment, classified into 9 categories, mostly similar to upregulated GO terms, but with different percentage and orders. Within the pathways analysis, Ag-NPs affected the endocytosis, *MAPK*, *TGF-β*, *p53* signalling pathways, pathways in cancer and *NFR2*-mediated oxidative stress response [55].

9.5 Toxicological Potential of Nanoparticles

The gene expression profiling of TiO_2-NPs of varying sizes and surface properties has been reported to induce pulmonary inflammation. However, the different TiO_2-NPs vary in the magnitude of the inflammatory response induced in a property-dependent manner [56]. Our recent studies demonstrated that TiO_2-NPs preferentially bind in subdomains IB, IIA of HSA and minor groove of DNA [57]. TiO_2-NPs might be able to enter the human stratum corneum and interact with the immune system. Silica NPs are used in the synthesis of cosmetics, foods, drugs, and printing ink tonners, on a large industrial scale. The nanotoxicity of crystalline silica causes chronic obstructive pulmonary diseases such as silicosis [58]. Silica NPs exists in the nature in many diverse forms [59, 60]. Fumed silica showed dose dependent accumulation of alveolar macrophages [61–63]. Cerium oxides (CeO_2)-NPs are one of the most widely used types for UV protection in paints or as fuel additives [64, 65]. CeO_2-NPs can be used as a scavenger of superoxide anions [66, 67]. CeO_2-NPs were shown to exhibit superoxide dismutase (SOD) and catalase enzymes mimetic activities in a redox-state dependent manner. CeO_2-NPs has been shown to hold the neuroprotective

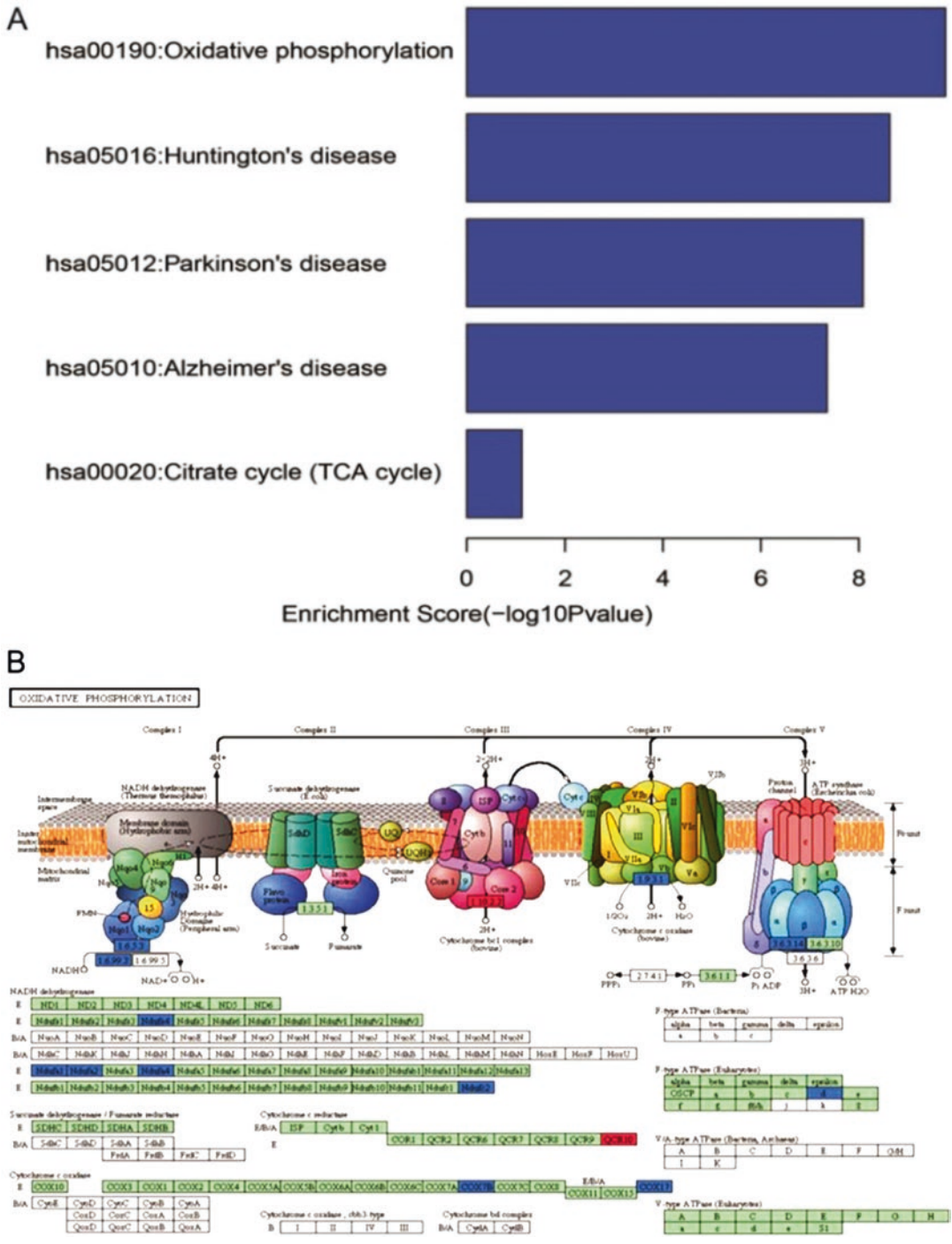

Fig. 9.8 (**a**) KEGG pathway enrichment analysis of mitochondria related genes. **a** A total of 27 mitochondria related genes were analyzed through DAVID functional annotation cluster tool. These genes mainly are involved in five KEGG pathways. (**b**) Oxidative phosphorylation is the most significant enrichment. **b** A schematic figure of the oxidative phosphorylation pathway by KEGG. mRNA microarray assay predicted up-regulated genes are stained red, and down-regulated genes are stained blue in this schematic figure (Reused from Fig. 9.2 of Li et al. [54] (Copyright and Permission granted from the Particle and Fibre Toxicology (http://creativecommons.org/licenses/by/4.0/), which permits unrestricted use, distribution, and reproduction in any medium, provided the original work is properly credited). (See the reference list for full citation of proper credited)

effects [68]. On the other hand, CeO_2-NPs has been reported to be cytotoxic to human hepatoma cells [69].

Ag-NPs have antimicrobial activity and are used in food packaging material, food supplements, odour-preventing textiles, cosmetics, kitchen utensils, toys, electronics, wound dressings, and room sprays [70]. Ag-NPs released Ag ions to exert antimicrobial properties by binding to sulphur- and phosphorous containing biomolecules and also causing damage to mammalian cells [71–75]. The in vivo inhalation data of Ag-NPs showing varied results from a minimal inflammatory response to the presence of inflammatory lesions in the lungs [76–79]. There are studies indicating that the dose-dependent increase of Ag-NPs might stimulate toxicity in the different organs [77, 78]. It has been hypothesized that small Ag-NPs will induce more prominent pulmonary toxicity compared to larger Ag particles because of the larger deposited dose in the alveoli and the higher dissolution rate. The dissolution of Ag-NPs depends on their particle size, the pH of the solution, the ions present in the solution [80–84]. The in vitro results show that the dissolution rate of the 15 nm Ag-NPs will probably be higher compared to the 410 nm Ag-NPs resulting in an increased ion release. None of the studies report complete dissolution of Ag-NPs, the effects observed after exposure to Ag-NPs can be induced by the released ions, the Ag-NPs itself or a combination of both [85]. Ag ions released from Ag-NPs caused more damage inside the nucleus as compared to Ag ions released from silver nitrate [86–88].

The harmful effects of carbon nanotubes (CNTs) to animals and cells appeared almost a decade ago [89]. Several mechanisms of toxicity, similar to the ones linked to asbestos-exposure, have been proposed for CNTs, such as (i) association of fibres with the cell membrane causing physical damage and cell membrane malfunction, (ii) protein-fibre interaction inhibiting protein function, and (iii) induction of ROS, either directly by the CNTs themselves or indirectly through mitochondrial dysfunctions or NADPH oxidase activation induced by so-called frustrated phagocytosis in e.g. macrophages [90–92]. It seems probable that a combination of different mechanisms could contribute to the toxicity of CNTs, as it has been considered to be the case with asbestos [93]. Multiwalled CNTs are efficient scavengers of $^{\bullet}OH$ and superoxide ($^{\bullet}O_2^-$) radicals in cell-free conditions [94]. The generation of free radicals by CNTs was suggested to be related to the amount and nature of defects in the CNTs, i.e. ruptures of the graphene framework [94]. In contrast, ROS formation by single walled CNTs was observed in cell media with and without FE1-Muta™ Mouse lung epithelial cells, at intermediate levels between that of Printex 90 and C60 fullerene and correlated with the order of genotoxicity [95]. Our toxicogenomic analysis on $ZnFe_2O_4$-NPs reveled its cytotoxicity and apoptosis through ROS generation and oxidative stress via *p53*, survivin, *bax/bcl-2* and caspase pathways in WISH cells [96]. We have also demonstrated that ZnO-NPs have the potential to induce DNA damage and alter the mitochondrial membrane potential of human lymphocytes [97]. Previously, we have reported that ZnO-QDs can induce dose dependent apoptosis induction in C2C12, HepG2 and MCF-7 cells via oxidative stress and alterations of apoptosis related genes [98, 99].

9.6 Conclusion and Future Perspective

The incessant use of NPs in various sectors and life domains may pose serious threats to ecosystem and adversely affect the living entities via interactions and accumulation of nanomaterials in the body of the organisms. Toxicogenomics approach notably contributes to our understanding of genetic changes at molecular levels. Significant change in the gene expression levels due to the NPs treatment provides information related to biochemical pathways and mechanism of action of nanotoxicants. Differential gene expression pattern may also yield molecular fingerprints of these nanotoxicants both with the in vitro and in vivo test model systems. Thus, the toxicogenomic methods have the power and potential to change nanotoxicology research landscape.

Acknowledgments SD gratefully acknowledge the financial support given by CSIR, New Delhi, India. The authors extend their appreciation to the International Scientific Partnership Program ISPP at King Saud University for funding this research work through ISPP# 0031.

References

1. Oberdorster G, Maynard A, Donaldson K et al (2005) A report from the ILSI Research Foundation/Risk Science Institute Nanomaterial Toxicity Screening Working Group. Principles for characterizing the potential human health effects from exposure: elements of screening strategy. Part Fibre Toxicol 6:2–8
2. Hoet PHM, Brüske-Hohlfeld I, Salata OV (2004) Nanoparticles: known and unknown health risks. J Nanobiotechnol 8:1–12
3. Salata O (2004) Applications of nanoparticles in biology and medicine. Nano Biotechnol 2:3
4. Wang K, Xu JJ, Chen HY (2005) A novel glucose biosensor based on the nanoscaled cobalt phthalocyanine-glucose oxidase biocomposite. Biosens Bioelectron 20:1388–1396
5. Yang MH, Jiang JH, Yang YH et al (2006) Carbon nanotube/cobalt hexacyanoferrate nanoparticle biopolymer system for the fabrication of biosensors. Biosens Bioelectron 21:1791–1797
6. Chen M, Zhang M, Borlak J et al (2012) A decade of toxicogenomic research and its contribution to toxicological science. Toxicol Sci 130:217–228
7. Ivask A, Bondarenko O, Jepihhina N et al (2010) Profiling of the reactive oxygen species-related ecotoxicity of CuO, ZnO, TiO_2, silver and fullerene nanoparticles using a set of recombinant luminescent Escherichia coli strains: differentiating the impact of particles and solubilised metals. Anal Bioanal Chem 398:701–716
8. Pujalté I, Passagne I, Brouillaud B et al (2011) Cytotoxicity and oxidative stress induced by different metallic nanoparticles on human kidney cells. Part Fibre Toxicol 8:10–26
9. Griffitt TJ, Weil R, Hyndman KA et al (2007) Exposure to copper nanoparticles causes injury and acute lethality in zebrafish (Danio rerio). Environ Sci Technol 41:8178–8186
10. Nair PMG, Choi J (2011) Characterization of a ribosomal protein L15 cDNA from Chironomus riparius (Diptera; Chironomidae): transcriptional regulation by cadmium and silver nanoparticles. Comp Biochem Physiol B Biochem Mol Biol 159:157–162
11. Oberdorster G, Oberdorster E, Oberdorster J (2005) Nanotoxicology: an emerging discipline evolving from studies of ultrafine particles. Environ Health Perspect 113(7):823–839
12. Donaldson K, Tran CL (2002) Inflammation caused by particles and fibers. Inhal Toxicol 14:5–27
13. Kumar A, Dhawan A (2013) Genotoxic and carcinogenic potential of engineered nanoparticles: an update. Arch Toxicol 87(11):1883–1900
14. Duan J, Yu Y, Li Y et al (2013) Cardiovascular toxicity evaluation of silica nanoparticles in endothelial cells and zebrafish model. Biomaterials 34(23):5853–5862
15. Khatri M, Bello D, Gaines P et al (2013) Nanoparticles from photocopiers induce oxidative stress and upper respiratory tract inflammation in healthy volunteers. Nanotoxicology 7(5):1014–1027
16. Shin JA, Lee EJ, Seo SM et al Nanosized titanium dioxide enhanced inflammatory responses in the septic brain of mouse. Neuroscience 165(2):445–454
17. Smita S, Gupta S, Bartonova A et al (2012) Nanoparticles in the environment: assessment using the causal diagram approach. Environ Health 11:S13
18. Chinta SJ, Andersen JK (2008) Redox imbalance in Parkinson's disease. Biochim Biophys Acta 1780(11):1362–1367
19. Husain M, Saber AT, Guo C et al (2013) Pulmonary instillation of low doses of titanium dioxide nanoparticles in mice leads to particle retention and gene expression changes in the absence of inflammation. Toxicol Appl Pharmacol 269:250–262
20. AshaRani P, Hande MP, Valiyaveettil S (2009) Anti-proliferative activity of silver nanoparticles. BMC Cell Biol 10:65
21. Kedziorek DA, Muja N, Walczak P et al (2010) Gene expression profiling reveals early cellular responses to intracellular magnetic labeling with superparamagnetic iron oxide nanoparticles. Magn Reson Med 63:1031–1043
22. Li X, He Q, Shi J (2014) Global gene expression analysis of cellular death mechanisms induced by mesoporous silica nanoparticle-based drug delivery system. ACS Nano 8:1309–1320
23. Foldbjerg R, Irving ES, Hayashi Y et al (2012) Global gene expression profiling of human lung epithelial cells after exposure to nanosilver. Toxicol Sci 130:145–157
24. Liu Y, Wang J (2013) Effects of DMSA-coated Fe3O4 nanoparticles on the transcription of genes related to iron and osmosis homeostasis. Toxicol Sci 131:521–536
25. Van Aerle R, Lange A, Moorhouse A et al (2013) Molecular mechanisms of toxicity of silver nanoparticles in zebrafish embryos. Environ Sci Technol 47(14):8005–8014
26. Andersen ME, Krewski D (2009) Toxicity testing in the 21st century: bringing the vision to life. Toxicol Sci 107(2):324–330
27. Yang H, Liu C, Yang D et al (2009) Comparative study of cytotoxicity, oxidative stress and genotoxicity induced by four typical nanomaterials: the role of particle size, shape and composition. J Appl Toxicol 29(1):69–78
28. Van Hummelen P, Sasaki J (2010) State-of-the-art genomics approaches in toxicology. Mutat Res 705(3):165–171

29. Wang Z, Gerstein M, Snyder M (2009) RNA-seq: a revolutionary tool for transcriptomics. Nat Rev Genet 10:57–63
30. Costa PM, Fadeel B (2016) Emerging systems biology approaches in nanotoxicology: towards a mechanism-based understanding of nanomaterial hazard and risk. Toxicol Appl Pharmacol 299:101–111
31. González-Ballester D, Casero D, Cokus S et al (2010) RNA-seq analysis of sulfur-deprived Chlamydomonas cells reveals aspects of acclimation critical for cell survival. Plant Cell 22:2058–2084
32. Miller R, Wu G, Deshpande RR et al (2010) Changes in transcript abundance in Chlamydomonas reinhardtii following nitrogen deprivation predict diversion of metabolism. Plant Physiol 154:1737–1752
33. Maier T, Guell M, Serrano L (2009) Correlation of mRNA and protein in complex biological samples. FEBS Lett 583:3966–3973
34. De Sousa Abreu R, Penalva LO, Marcotte E et al (2009) Global signatures of protein and mRNA expression levels. Mol BioSyst 5:1512–1526
35. Simon DF, Domingos RF, Hauser C et al (2013) Transcriptome sequencing (RNA-seq) analysis of the effects of metal nanoparticle exposure on the transcriptome of Chlamydomonas reinhardtii. Appl Environ Microbiol 79(16):4774–4785
36. Lucafò M, Gerdol M, Pallavicini A et al (2013) Profiling the molecular mechanism of fullerene cytotoxicity on tumor cells by RNA-seq. Toxicology 314(1):183–192. https://doi.org/10.1016/j.tox.2013.10.001
37. Yang H, Kozicky L, Saferali A et al (2016) Endosomal pH modulation by peptide-gold nanoparticle hybrids enables potent anti-inflammatory activity in phagocytic immune cells. Biomaterials 111:90–102. https://doi.org/10.1016/j.biomaterials.2016.09.032
38. Ambrosone A, Scotto di Vettimo MR, Malvindi MA et al (2014) Impact of amorphous SiO2 nanoparticles on a living organism: morphological, behavioral, and molecular biology implications. Front Bioeng Biotechnol 2:37
39. Tian JH, Hu JS, Li FC et al (2016) Effects of TiO_2 nanoparticles on nutrition metabolism in silkworm fat body. Biol Open 5(6):764–769. https://doi.org/10.1242/bio.015610
40. Novo M, Lahive E, Díez-Ortiz M et al (2015) Different routes, same pathways: molecular mechanisms under silver ion and nanoparticle exposures in the soil sentinel *Eisenia fetida*. Environ Pollut 205:385–393
41. Mitra M, Dilnawaz F, Misra R et al (2011) Toxicogenomics of nanoparticulate delivery of etoposide: potential impact on nanotechnology in retinoblastoma therapy. Cancer Nanotechnol 2(1–6):21–36
42. Chou CC, Hsiao HY, Hong QS et al (2008) Single-walled carbon nanotubes can induce pulmonary injury in mouse model. Nano Lett 8(2):437–445
43. Lim DH, Jang J, Kim S et al (2012) The effects of sub-lethal concentrations of silver nanoparticles on inflammatory and stress genes in human macrophages using cDNA microarray analysis. Biomaterials 33(18):4690–4699
44. Waters KM, Masiello LM, Zangar RC et al (2009) Macrophage responses to silica nanoparticles are highly conserved across particle sizes. Toxicol Sci 107(2):553–569
45. Zhang L, Wang X, Zou J et al (2015) Effects of an 11-nm DMSA-coated iron nanoparticle on the gene expression profile of two human cell lines, THP-1 and HepG2. J Nanobiotechnol 13:3. https://doi.org/10.1186/s12951-014-0063-3
46. Ding L, Stilwell J, Zhang T et al (2005) Molecular characterization of the cytotoxic mechanism of multiwall carbon nanotubes and nano-onions on human skin fibroblast. Nano Lett 5(12):2448–2464
47. Long TC, Tajuba J, Sama P et al (2007) Nanosize titanium dioxide stimulates reactive oxygen species in brain microglia and damages neurons in vitro. Environ Health Perspect 115(11):1631–1637
48. Van der Zande M, Vandebriel RJ, Groot MJ et al (2014) Sub-chronic toxicity study in rats orally exposed to nanostructured silica. Part Fibre Toxicol 11:8
49. Osmond-McLeod MJ, Oytam Y, Rowe A et al (2016) Long-term exposure to commercially available sunscreens containing nanoparticles of TiO_2 and ZnO revealed no biological impact in a hairless mouse model. Part Fibre Toxicol 13(1):44
50. Busch W, Kühnel D, Schirmer K et al (2010) Tungsten carbide cobalt nanoparticles exert hypoxia-like effects on the gene expression level in human keratinocytes. BMC Genomics 11:65
51. Pisani C, Gaillard JC, Nouvel V et al (2015) High-throughput, quantitative assessment of the effects of low-dose silica nanoparticles on lung cells: grasping complex toxicity with a great depth of field. BMC Genomics 16:315
52. Fisichella M, Berenguer F, Steinmetz G et al (2014) Toxicity evaluation of manufactured CeO2 nanoparticles before and after alteration: combined physicochemical and whole-genome expression analysis in Caco-2 cells. BMC Genomics 15:700
53. Fisichella M, Berenguer F, Steinmetz G et al (2012) Intestinal toxicity evaluation of TiO2 degraded surface-treated nanoparticles: a combined physicochemical and toxicogenomics approach in caco-2 cells. Part Fibre Toxicol 9:18
54. Li X, Zhang C, Zhang X et al (2016) An acetyl-L-carnitine switch on mitochondrial dysfunction and rescue in the metabolomics study on aluminum oxide nanoparticles. Part Fibre Toxicol 13:4. https://doi.org/10.1186/s12989-016-0115-y
55. Sahu SC, Zheng J, Yourick JJ et al (2015) Toxicogenomic responses of human liver HepG2 cells to silver nanoparticles. J Appl Toxicol 35(10):1160–1168
56. Halappanavar S, Saber AT, Decan N et al (2015) Transcriptional profiling identifies physicochemical properties of nanomaterials that are determinants

of the in vivo pulmonary response. Environ Mol Mutagen 56:245–264
57. Ali K, Qais FA, Dwivedi S et al (2017) Titanium dioxide nanoparticles preferentially bind in subdomains IB, IIA of HSA and minor groove of DNA. J Biomol Struct Dyn. https://doi.org/10.1080/07391102.2017.1361339
58. Colvin VL (2003) The potential environmental impact of engineered nanomaterials. Nat Biotechnol 21(10):1166–1170
59. Mohamed BM, Verma NK, Prina-Mello A et al (2011) Activation of stress-related signalling pathway in human cells upon SiO_2 nanoparticles exposure as an early indicator of cytotoxicity. J Nanobiotechnol 9:29
60. Perkins TN, Shukla A, Peeters PM et al (2012) Differences in gene expression and cytokine production by crystalline vs. amorphous silica in human lung epithelial cells. Part Fibre Toxicol 9(1):6
61. Reuzel PG, Bruijntjes JP, Feron VJ et al (1991) Subchronic inhalation toxicity of amorphous silicas and quartz dust in rats. Food Chem Toxicol 29(5):341–354
62. Xu Z, Wang SL, Gao HW (2010) Effects of nanosized silicon dioxide on the structures and activities of three functional proteins. J Hazard Mater 180(1–3):375–383
63. Rabolli V, Thomassen LC, Princen C et al (2010) Influence of size, surface area and microporosity on the in vitro cytotoxic activity of amorphous silica nanoparticles in different cell types. Nanotoxicology 4(3):307–318
64. Salata O (2004) Applications of nanoparticles in biology and medicine. J Nanobiotechnol 2:3
65. Pirmohamed T, Dowding JM, Singh S et al (n.d.) Nanoceria exhibit redox state dependent catalase mimetic activity. Chem Commun (Camb) 46:2736–2738
66. Heckert EG, Karakoti AS, Seal S et al (2008) The role of cerium redox state in the SOD mimetic activity of nanoceria. Biomaterials 29:2705–2709
67. Kong L, Cai X, Zhou X et al (2011) Nanoceria extend photoreceptor cell lifespan in tubby mice by modulation of apoptosis/survival signaling pathways. Neurobiol Dis 42:514–523
68. Schubert D, Dargusch R, Raitano J et al (2006) Cerium andyttrium oxide nanoparticles are neuroprotective. Biochem Biophys Res Commun 342:86–91
69. Cheng G, Guo W, Han L et al (2013) Cerium oxide nanoparticles induce cytotoxicity in human hepatoma SMMC-7721 cells via oxidative stress and the activation of MAPK signaling pathways. Toxicol in Vitro 27:1082–1088
70. Wijnhoven SWP, Peijnenburg WJGM, Herberts CA et al (2009) Nano-silver – a review of available data and knowledge gaps in human and environmental risk assessment. Nanotoxicology 3:109–138
71. Sotiriou GA, Pratsinis SE (2010) Antibacterial activity of nanosilver ions and particles. Environ Sci Technol 44:5649–5654
72. Sotiriou GA, Pratsinis SE (2011) Engineering nanosilver as an antibacterial, biosensor and bioimaging material. Curr Opin Chem Eng 1(1):3–10
73. Dwivedi S, Saquib Q, Al-Khedhairy AA et al (2015) Rhamnolipids functionalized AgNPs-induced oxidative stress and modulation of toxicity pathway genes in cultured MCF-7 cells. Colloids Surf B: Biointerfaces 132:290–298
74. Morones JR, Elechiguerra JL, Camacho A et al (2005) The bactericidal effect of silver nanoparticles. Nanotechnology 16:2346–2353
75. Xiu ZM, Zhang QB, Puppala HL et al (2012) Negligible particle specific antibacterial activity of silver nanoparticles. Nano Lett 12:4271–4275
76. Stebounova LV, Adamcakova-Dodd A, Kim JS et al (2011) Nanosilver induces minimal lung toxicity or inflammation in a subacute murine inhalation model. Part Fibre Toxicol 8:5
77. Song KS, Sung JH, Ji JH et al (2012) Recovery from silver-nanoparticle exposure- induced lung inflammation and lung function changes in Sprague Dawley rats. Nanotoxicology 7:169–180
78. Sung JH, Ji JH, Yoon JU et al (2008) Lung function changes in Sprague–Dawley rats after prolonged inhalation exposure to silver nanoparticles. Inhal Toxicol 20:567–574
79. Sung JH, Ji JH, Park JD et al (2009) Subchronic inhalation toxicity of silver nanoparticles. Toxicol Sci 108:452–461
80. Ma R, Levard C, Marinakos SM et al (2012) Size-controlled dissolution of organic-coated silver nanoparticles. Environ Sci Technol 46:752–759
81. Leo BF, Chen S, Kyo Y et al (2013) The stability of silver nanoparticles in a model of pulmonary surfactant. Environ Sci Technol 47:11232–11240
82. Stebounova LV, Guio E, Grassian VH (2011) Silver nanoparticles in simulated biological media: a study of aggregation, sedimentation, and dissolution. J Nanopart Res 13:12
83. Kent RD, Vikesland PJ (2012) Controlled evaluation of silver nanoparticles dissolution using atomic force microscopy. Environ Sci Technol 46:6977–6984
84. Zook JM, Long SE, Cleveland D et al (2011) Measuring silver nanoparticle dissolution in complex biological and environmental matrices using UV-visible absorbance. Anal Bioanal Chem 401:1993–2002
85. Pratsinis A, Hervella P, Leroux JC et al (2013) Toxicity of silver nanoparticles in macrophages. Small 9:2576–2584
86. Lubick N (2008) Nanosilver toxicity: ions, nanoparticles–or both? Environ Sci Technol 42:8617
87. Park EJ, Yi J, Kim Y et al (2010) Silver nanoparticles induce cytotoxicity by a Trojan-horse type mechanism. Toxicol in Vitro 24:872–878
88. Limbach LK, Wick P, Manser P et al (2007) Exposure of engineered nanoparticles to human lung epithelial cells: influence of chemical composition and catalytic activity on oxidative stress. Environ Sci Technol 41:4158–4163

89. Lam CW, James JT, McCluskey R et al (2004) Pulmonary toxicity of singlewall carbon nanotubes in mice 7 and 90 days after intratracheal instillation. Toxicol Sci 77:126–134
90. Sargent L, Reynolds S, Castranova V (2010) Potential pulmonary effects of engineered carbon nanotubes: in vitro genotoxic effects. Nanotoxicology 4:396–408
91. Shvedova AA, Pietroiusti A, Fadeel B et al (2012) Mechanisms of carbon nanotube-induced toxicity: focus on oxidative stress. Toxicol Appl Pharmacol 261:121–133
92. Sund J, Alenius H, Vippola M et al (2011) Proteomic characterization of engineered nanomaterial–protein interactions in relation to surface reactivity. ACS Nano 5:4300–4309
93. Jaurand MC, Renier A, Daubriac J (2009) Mesothelioma: do asbestos and carbon nanotubes pose the same health risk? Part Fibre Toxicol 6:1–14
94. Fenoglio I, Greco G, Tomatis M et al (2008) Structural defects play a major role in the acute lung toxicity of multiwall carbon nanotubes: physicochemical aspects. Chem Res Toxicol 21:1690–1697
95. Jacobsen NR, Pojana G, White P et al (2008) Genotoxicity, cytotoxicity, and reactive oxygen species induced by single-walled carbon nanotubes and C60 fullerenes in the FE1-Muta™Mouse lung epithelial cells. Environ Mol Mutagen 49:476–487
96. Saquib Q, Al-Khedhairy AA, Ahmad J et al (2013) Zinc ferrite nanoparticles activate IL-1b, NFKB1, CCL21 and NOS2 signaling to induce mitochondrial dependent intrinsic apoptotic pathway in WISH cells. Toxicol Appl Pharmacol 273(2):289–297
97. Musarrat J, Saquib Q, Azam A et al (2009) Zinc oxide nanoparticles-induced DNA damage in human lymphocytes. Int J Nanopart 2(1/2/3/4/5/6):402–415
98. Wahab R, Khan F, Yang YB et al (2016) Zinc oxide quantum dots: multifunctional candidates for arresting the C2C12 cancer cells and their role towards caspase 3 and 7 genes. RSC Adv 6:26111–26120
99. Wahab R, Siddiqui MA, Saquib Q et al (2014) ZnO nanoparticles induced oxidative stress and apoptosis in HepG2 and MCF-7 cancer cells and their antibacterial activity. Colloids Surf B: Biointerfaces 117:267–276